Available online at www.sciencedirect.com
ScienceDirect
Procedia Materials Science 3 (2014) 2117 – 2121
Procedia Materials Science
www.elsevier.com/locate/procedia

20th European Conference on Fracture (ECF20)

Nonlinear constitutive model and finite element analysis of damage processes in ferroelectrics

R. Gellmann*, A. Ricoeur

Institute of Mechanics, Department of Mechanical Engineering, University of Kassel, Moenchebergstr. 7, 34125 Kassel, Germany

Abstract

In this paper a damage model for ferroelectric materials is presented. It is implemented in terms of a user element in a commercial FEM-code Abaqus. The model is based on micromechanical considerations of domain switching and its interaction with microcrack growth and coalescence. The influence of damage evolution on the effective material properties is demonstrated. Further, a finite element analysis of a multilayer actuator is performed, showing damage and crack patterns.

Selection and peer-review under responsibility of the Norwegian University of Science and Technology (NTNU), Department of Structural Engineering

Keywords: Ferroelectrics; Polarization switching; Multilayer actuator; Damage model

1. Introduction

Ferroelectric materials as components of smart structures are widely used in e.g. actuators, acoustic sensors as well as in airfoil control systems. Due to the brittleness of these materials, fracture mechanical approaches are playing an essential role in the modern research. Depending on the application, the material is subjected to mechanical, electrical or combined electromechanical loading. The mechanics of these materials is significantly determined by irreversible nonlinear ferroic effects arising on the microscopic scale, such as polarization switching. These switching processes are accompanied by internal stresses due to the strain incompatibility between neighboring grains, which results in damage and thus a significant variation of the material properties (Gellmann et al., 2013). That means that a comprehensive ferroelectric material model should consider fracture and damage mechanical approaches. Besides that, the long term reliability of smart structures requires the application of numerical tools predicting crack initiation and growth under electromechanical loading conditions.

* Corresponding author. Tel.: +49-561-804-2824 ; fax: +49-561-804-2720.
E-mail address: gellmann@uni-kassel.de

Selection and peer-review under responsibility of the Norwegian University of Science and Technology (NTNU), Department of Structural Engineering
doi:10.1016/j.mspro.2014.06.342

2. Micromechanical Model

The nonlinear effects are modelled by decomposing the strain ϵ_{ij} and electric displacement D_i additively into a linear piezoelectric part denoted with a superscript *rev* and a remanent strain $\epsilon_{ij}^{\mathrm{irr}}$ and remanent polarization P_i^{irr} emerging due to polarization switching phenomena

$$\epsilon_{ij} = \epsilon_{ij}^{\mathrm{rev}} + \epsilon_{ij}^{\mathrm{irr}}, \qquad D_i = D_i^{\mathrm{rev}} + P_i^{\mathrm{irr}}. \tag{1}$$

The remanent parts are functions of the load history and remain after switching off the electric field and mechanical stress. The domain switching is simulated by applying a multidomain switching model of polycrystalline ferroelectrics, as illustrated in Fig. 1. Four possible domain species are assumed with $\nu^{(N)}$ being the volume fraction of the N^{th} domain within the representative volume element (RVE). The volume fractions satisfy the following relation

$$\sum_{N=1}^{4} \nu^{(N)} = 1, \qquad 0 \le \nu^{(N)} \le 1. \tag{2}$$

The ferroelectric model is based on a thermodynamical potential

$$\Psi(\epsilon_{kl}, E_i) = \frac{1}{2} C_{ijkl}\epsilon_{ij}\epsilon_{kl} - e_{ikl}\epsilon_{kl}E_i - \frac{1}{2}\kappa_{ij}E_iE_j - C_{ijkl}\epsilon_{ij}^{\mathrm{irr}}\epsilon_{kl} + e_{ikl}\epsilon_{kl}^{\mathrm{irr}}E_i - P_i^{\mathrm{irr}}E_i \tag{3}$$

leading to the macroscopic constitutive law in a RVE

$$\sigma_{ij} = \left.\frac{\partial\Psi(\epsilon_{kl}, E_i)}{\partial\epsilon_{kl}}\right|_{E_i} = C_{ijkl}(\epsilon_{kl} - \epsilon_{kl}^{\mathrm{irr}}) - e_{kij}E_k, \tag{4}$$

$$D_i = -\left.\frac{\partial\Psi(\epsilon_{kl}, E_i)}{\partial E_i}\right|_{\epsilon_{kl}} = e_{ikl}(\epsilon_{kl} - \epsilon_{kl}^{\mathrm{irr}}) + \kappa_{ik}E_k + P_i^{\mathrm{irr}}. \tag{5}$$

Here, ϵ_{ij}, σ_{ij}, E_i and D_k are respectively the components of the total strain, local stress tensor, electric field and electric displacement vector. C_{ijkl}, e_{ikl}, κ_{ij} are respectively the effective elastic, piezoelectric and the dielectric constants, which depend on the current configuration of domain structure in the RVE. They are obtained by averaging over all domains within an RVE

$$C_{ijkl} = \sum_{N=1}^{4} C_{ijkl}^{(N)}\nu^{(N)}, \qquad e_{ijk} = \sum_{N=1}^{4} e_{ijk}^{(N)}\nu^{(N)}, \qquad \kappa_{ij} = \sum_{N=1}^{4} \kappa_{ij}^{(N)}\nu^{(N)}. \tag{6}$$

For small deformations, the strain tensor and electric field are calculated from the displacement gradient and the gradient of the scalar potential, respectively

$$\epsilon_{ij} = (u_{i,j} + u_{j,i})/2, \qquad E_i = -\varphi_{,i}. \tag{7}$$

Within each domain, the polarisation vector P_i is assumed to switch as soon as mechanical and electrical energy reduction exceeds a critical energy barrier $w_{\mathrm{crit}}^{\gamma}$, see Hwang et al. (1995). The switching is interpreted as the rotation of the polarization vector around the out-of-plane axis, see Fig. 1. The evolution law for the change of internal variables $\dot{\nu}_N$ reads

$$w_{\mathrm{diss}}^{\gamma(N)} = \sigma_{ij}\Delta\epsilon_{ij}^{\gamma(N)} + E_i\Delta P_i^{\gamma(N)}, \qquad \dot{\nu}_N = -\dot{\nu}_N^0\mathcal{H}\left(\frac{w_{\mathrm{diss}}^{\gamma(N)}}{w_{\mathrm{crit}}^{\gamma}} - 1\right), \tag{8}$$

where $\dot{\nu}_N^0$ is a model parameter and different switching variants $\gamma = \pm 90°, 180°$ are distinguished. Here, $w_{\mathrm{diss}}^{\gamma(N)}$ is the sum of mechanical and electrical work per unit volume for the N^{th} domain species and $w_{\mathrm{crit}}^{\gamma}$ corresponds to the minimal energy required for domain switching, such that $w_{\mathrm{crit}}^{\pm 90°} = \sqrt{2}E_C P^0$, and $w_{\mathrm{crit}}^{180°} = 2E_C P^0$. In Eq. (8) a generalized Reuss approximation is implied. That is, the mechanical stresses and the electric field components are assumed to be constant

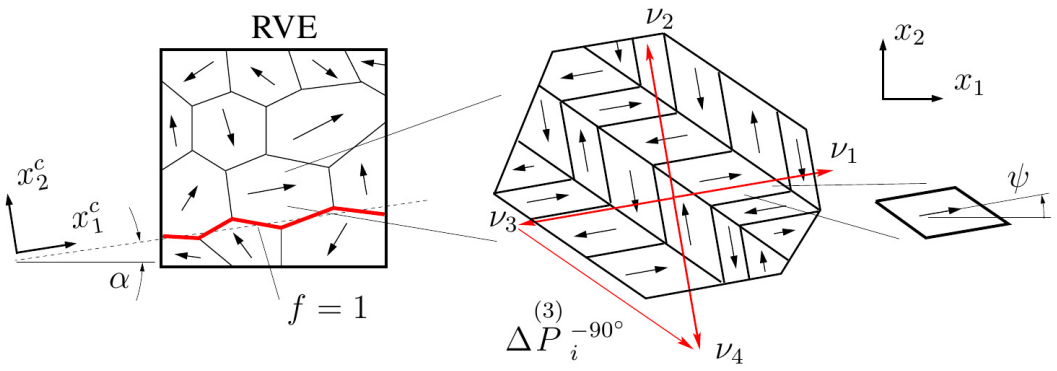

Fig. 1. Schematic illustration of an RVE, a single polycrystalline grain with 4 possible tetragonal domain species and a single domain with poling direction ψ in the (x_1, x_2) plane.

and are not modified by the switching events. The local coordinates of the spontaneous strain $\Delta\epsilon_{ij}^{\gamma(N)}$ and change of polarisation $\Delta P_i^{\gamma(N)}$ are described by $\epsilon_D = (c-a)/a_0$

$$\Delta\epsilon_{ij}^{\pm 90^\circ} = \epsilon_D \begin{pmatrix} 1 & 0 \\ 0 & -1 \end{pmatrix}, \qquad \Delta\epsilon_{ij}^{180^\circ} = 0, \tag{9}$$

$$\Delta P_k^{+90^\circ} = P^0 \begin{pmatrix} -1 \\ 1 \end{pmatrix}, \quad \Delta P_k^{-90^\circ} = P^0 \begin{pmatrix} -1 \\ -1 \end{pmatrix}, \quad \Delta P_k^{180^\circ} = P^0 \begin{pmatrix} -2 \\ 0 \end{pmatrix}. \tag{10}$$

The changes of remanent strain and polarization induced by domain switching are calculated by building a sum over all switching events weighted by the change of the corresponding volume fraction $dv^{(N)}$, such that

$$\mathrm{d}\epsilon_{ij}^{\mathrm{irr}} = \sum_{N=1}^{4} \Delta\epsilon_{ij}^{\gamma(N)} \mathrm{d}v^{(N)}, \qquad \mathrm{d}P_i^{\mathrm{irr}} = \sum_{N=1}^{4} \Delta P_i^{\gamma(N)} \mathrm{d}v^{(N)}. \tag{11}$$

Note, once the polarization switches, the irreversible strain is locked and cannot be reverse-switched unless external loads enforce it.

The above outlined model is implemented into a FE algorithm by introducing two additional terms on the right-hand side of the algebraic system of equations, $\{f_e\}$ and $\{q_e\}$, such that

$$[K_{uu}]\{u\} + [K_{u\varphi}]\{\varphi\} = \{f\} + \{f_e\}, \tag{12}$$

$$[K_{\varphi u}]\{u\} + [K_{\varphi\varphi}]\{\varphi\} = \{q\} + \{q_e\}. \tag{13}$$

The additional terms describe the residual stresses and spontaneous polarization due to domain wall motion and are calculated as follows

$$\{f_e\} = \int_{V^E} [B_u]^{\mathrm{T}} [C]\{\epsilon^{\mathrm{irr}}\} \mathrm{d}V, \qquad \{q_e\} = \int_{V^E} [B_\varphi]^{\mathrm{T}} ([e]\{\epsilon^{\mathrm{irr}}\} - \{P^{\mathrm{irr}}\}) \mathrm{d}V. \tag{14}$$

Here, the matrices $[B_u]$ and $[B_\varphi]$ relate the nodal variables $\{u\}$ and $\{\varphi\}$ with strain and electric field, in accordance with Eq. (7). The generalized stiffness matrices are given as follows

$$[K_{uu}] = \int_{V^E} [B_u]^T [C][B_u] \mathrm{d}V, \quad [K_{\varphi\varphi}] = -\int_{V^E} [B_\varphi]^T [\kappa]^T [B_\varphi] \mathrm{d}V, \quad [K_{u\varphi}] = [K_{\varphi u}]^T = \int_{V^E} [B_u]^T [e]^T [B_\varphi] \mathrm{d}V. \tag{15}$$

Now, the effective properties of damaged ferroelectric materials are calculated. The constitutive law, as given by Eqs. (4) and (5) is still valid. However, the material constants are modified by the damage. Therefore, a general relation between the volume averages of two piezoelectric field variables Π and Z is considered as

$$\langle Z\rangle = F^{\star}\langle\Pi\rangle, \tag{16}$$

with $\Pi = (\sigma_{11}, \sigma_{22}, \sigma_{12}, D_1, D_2)^{\mathrm{T}}$, and $Z = (\epsilon_{11}, \epsilon_{22}, 2\epsilon_{12}, -E_1, -E_2)^{\mathrm{T}}$. Here, $F^{\star}$ is the generalized compliance. Moreover, Eq. (16) can be written in an equivalent constitutive formulation with strain and electric field being independent variables $\langle\Pi\rangle = C^{\star}\langle Z\rangle$. The average strain and electric field density can be decomposed into two parts $\langle Z\rangle = Z^{\mathrm{M}} + Z^{\mathrm{C}}$ with $Z^{\mathrm{M}} = F^{\mathrm{M}}\Pi^0$ representing the matrix and $Z^{\mathrm{C}} = F^{\mathrm{C}}\Pi^0$ the defect phase. Here, $\langle\Pi\rangle = \Pi^0$ are the external loads. Then, it can be shown that the generalized compliance $F^{\star}$ as well as $C^{\star}$ are given as the sum of the generalized compliance of the matrix medium $F^{\mathrm{M}} = [C^{\mathrm{M}}]^{-1}$ and a contribution to be determined through the crack surface deformation F^{C}, i.e. $F^{\star} = F^{\mathrm{M}} + F^{\mathrm{C}}$. The contribution of micro cracks to the averaged strain and el. field density Z^{C} is given by

$$\epsilon_{ij}^{\mathrm{C}} = \frac{1}{2A}\int_{-a}^{+a}(\Delta u_i n_j + \Delta u_j n_i)\,\mathrm{d}x_1^c, \qquad E_i^{\mathrm{C}} = -\frac{1}{A}\int_{-a}^{+a}\Delta\varphi\, n_i\,\mathrm{d}x_1^c. \tag{17}$$

The calculations are done by applying the so called dilute model where defect interaction is neglected. Jumps of the displacement and the electric potential across crack surfaces are given by

$$\Delta u_M = 2Y_{MN}\sqrt{a^2 - (x_1^c)^2}\,\Pi_{N2}. \tag{18}$$

The latter is drawn from a closed form solution of the piezoelectric Griffith crack problem (Ricoeur and Kuna, 2003). This means, that the crack is assumed to be in a flawless matrix medium. Here, Y_{MN} is the Irwin matrix. Note that Eqs. (17) and (18) are given in the coordinate system of a microcrack (x_1^c, x_2^c). After calculating F^C, the material properties in Eqs. (14) and (15) are updated according to

$$C^{\star} = [(C^{\mathrm{M}})^{-1} + F^{\mathrm{C}}]^{-1}. \tag{19}$$

The influence of damage evolution is governed by a damage parameter $f = 4a^2/A$ which describes the density of microcracks, that is $f = 0$ for a flawless material and $f = 1$ for the full damage. The microcrack initiation is controlled by a mode-I stress intensity factor $K_I = K_{IC}$, where $K_I = \sqrt{\pi a_n}\sigma_I$ and σ_I is the maximal principal stress. Once the criterion is satisfied the microcrack is initiated and the calculation continues with crack growth, such that $a_n = a_0 + n\cdot\Delta a$ and $f_n = f_0 + n\cdot\Delta f$, where a_n is the crack length associated with the damage parameter f_n.

3. Example

The constitutive model has been implemented into the commercial FEM-code Abaqus in terms of a user element. To show an example, the geometry of specimen used in laboratory experiments by Shindo et al. (2004) has been chosen. Fig. 2 shows the sample which is a multilayer actuator consisting of four $BaTiO_3$ piezoelectric ceramic layers, alternating with surface and internal electrodes. The dimensions of the specimen in mm units are also shown in Fig. 2.

The computational results are presented in Figs. 3 and 4, showing an excerpt around an internal electrode. Polarization vectors are presented in Fig. 3 at the end of the poling process with $E_{\max} = 5E_c$ corresponded to a layer thikness of 5 mm. Maximal principal stresses are shown in Fig. 4. Those are largest close to the electrode tips leading to crack initiation and damage of the actuator. This is because of the high concentration of induced electric field and associated inelastic strain near the electrode tips. The results provided in Fig. 4 give useful information for the damage analysis of advanced piezoelectric devices, although the damage model depicted in section 2 has not yet been included in the simulations.

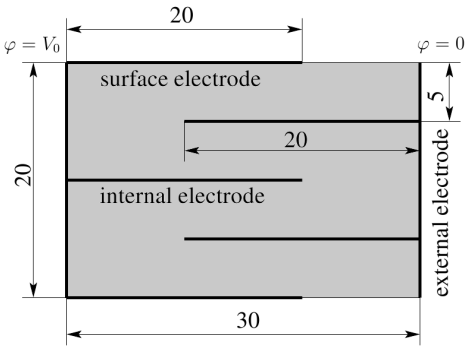

Fig. 2. Geometry and electric boundary conditions of the computational model of a multilayer actuator. The dimensions of the specimen are given in mm units.

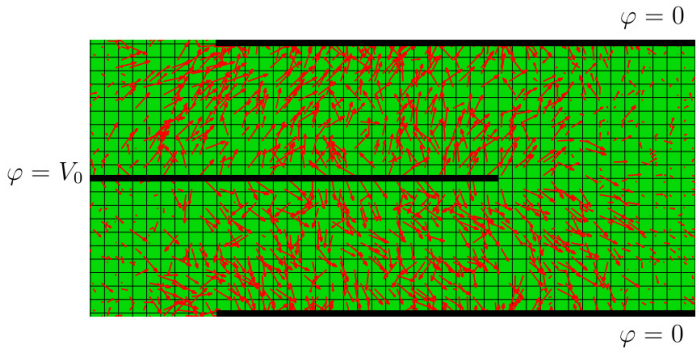

Fig. 3. Polarization vectors around electodes inside actuator after poling process.

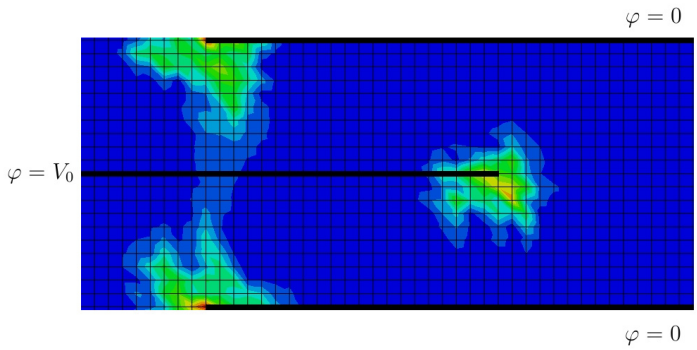

Fig. 4. Maximal principal stresses at the electrode tips during polarization process: red color (100 MPa), green color (35 MPa).

References

Gellmann, R., Ricoeur, A., Merkel, E., Wang Z., 2013. Generalized boundary conditions and effective properties in cracked piezoelectric solids. PAMM 13, 225–226.

Hwang, S.C., Lynch, C.S., McMeeking, R.M., 1995. Ferroelectric/ferroelastic interactions and a polarization switching model. Acta Metallurgica et Materialia 43(5), 2073–2084.

Ricoeur, A., Kuna, M., 2003. Influence of electric fields on the fracture of ferroelectric ceramics. Journal of the European Ceramic Society 23, 1313–1328.

Shindo, Y., Yoshida, M., Narita, F., Horiguchi, K., 2004. Electroelastic field concentrations ahead of electrodes in multilayer piezoelectric actuators: experiment and finite element simulation. Journal of the Mechanics and Physics of Solids 52, 1109–1124.